Modeling of a Liquid-Propellant Heat-Sink Rocket Engine

ME448/548: Final Project
Marc Wasserman
March 20, 2020

Introduction

The Portland State Aerospace Society (PSAS) is developing an alcohol-liquid oxygen rocket engine to power its next generation LV-4 rocket. PSAS previous attempted to build a fully-functional, small scale prototype but encountered difficulties with the cooling channels, rendering the entire 3d engine inoperable. To allow for testing of the thrust and combustion chamber with minimal added complexity, PSAS is now developing a heat-sink engine without any active cooling. This type of engine is generally understood to only be suitable for firings of a few seconds [1], however this should be enough to validate the design.

Because the expected engine combustion temperature is expected to be about 3100K, one of the key challenges of a heat sink engine is determining how long it can be tested before the engine wall melts. PSAS is currently weighing whether to use a cheaper Aluminum or a more expensive stainless steel for the engine. The goal of this project is to create a CFD simulation using Star CCM+ that simulates the proposed engine design and determines how the choice of material will affect the amount of time an engine can be fired before melting occurs.

Physical Model and Boundary Conditions

Rocket Parameters

At its most basic, a rocket engine is an application of the classic converging-diverging nozzle which compresses subsonic flow through a constriction, creates choked flow at the narrowest point and allows for supersonic expansion through the bell. The important parameters of a rocket engine are its thrust, chamber pressure, stagnation temperature, mass flow rate, throat area and exit area. These values, shown below in Table 1, have been determined by other work at PSAS and have been used to create the rocket profile used for this simulation.

Table 1: Rocket parameters for the test engine. Most values provided by PSAS design optimization work [2].

Parameter	Metric	US
Desired thrust	6 kN	1350 lbf
Mass flow rate	2.62 kg/s	5.76 lb/s
Chamber pressure	2.41 MPa	350 psi
Chamber temperature	3100 K	5580 R
Chamber cross-section area	9.13e-3 m^2	14.2 in^2
Throat area	1.83e-3 m^2	2.835 in^2
Exit area	8.35e-3 m^2	12.94 in^2

The rocket engine used for this simulation is shown below in Figure 1. This engine has been designed by PSAS using the theoretical rocket equations described in Huzel & Huang and combustion parameters from CEARun, a combustion analysis program created by NASA.

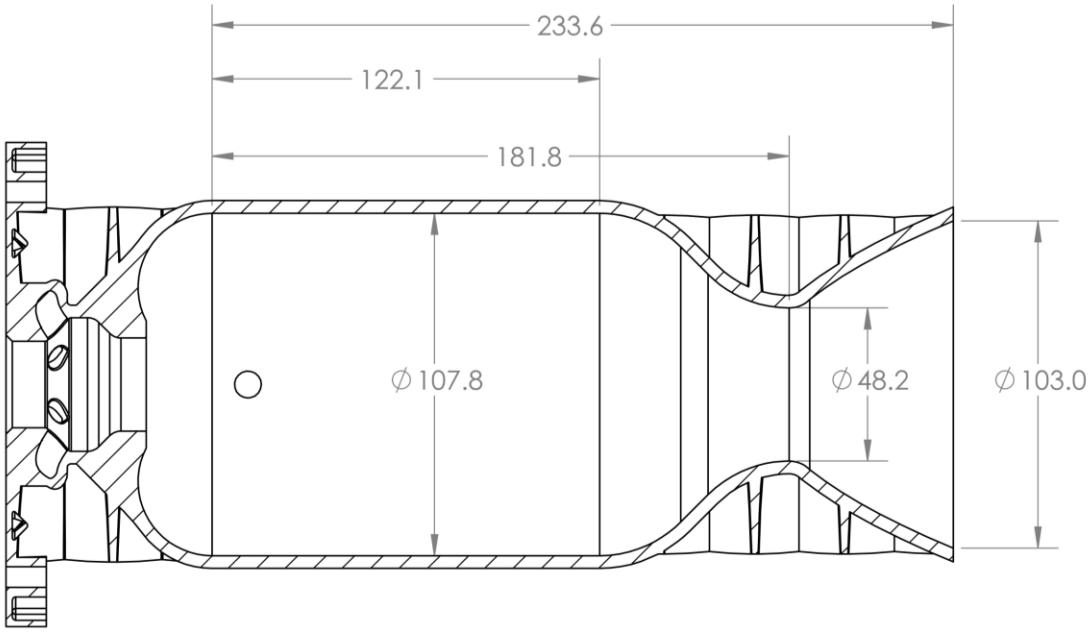

Figure 1: PSAS heat sink rocket engine prototype cut section. Dimensions are in mm. The section used in the CFD model extends from the start of the straight section on the left to the end of the bell on the right.

Key Equations & Assumptions

An important simplification for this simulation is that air is used in the model instead of actual combustion products. This is done because the properties of air are well established and its material properties are part of the standard Star CCM+ library. Because gases tend to act more like ideal gases at high temperatures, air is expected to be a reasonable analogue for the actual combustion products.

Some of the key equations used to determine the expected flow behavior and validate the simulation outputs include:

- *Dynamic viscosity of air:* $\mu = 1.46x10^{-6}\left[\frac{T^{3/2}}{T+111}\right] Ns/m^2$ [4]
- *Density of an ideal gas:* $\rho = \frac{P}{RT}$ [4]
- *Reynolds number:* $Re = \frac{\rho VD}{\mu}$ [5]
- *Speed of sound in an ideal gas:* $c = \sqrt{RTk}$ [4]
- *Pressure ratio (isentropic flow):* $p^* = p_0\left[\frac{2}{k+1}\right]^{k/(k-1)}$ [4]
- *Diffusion time scale:* $t^* = \frac{L^2}{\alpha}$

These equations are solved below in Table 2. The Reynolds number found is used to determine whether a turbulent or laminar model is most appropriate, the time scale guides the choice of time step, and the remaining values are used to compare the hand calculations to the simulation results.

Table 2: Fluid parameters for the CFD Model. For this model, air is used instead of the actual combustion products.

Parameter	Value
Temperature [2]	3100K
Air density	2.708 kg/m^3
Gas constant for air [3]	287 J/kgK
Chamber diameter	0.1078 m
Throat diameter	0.0483 m
Velocity through chamber	9.13e-3 m^2
Air dynamic viscosity, 3100K	7.8e-5 Ns/m^2
Reynolds number	3.78e5
Speed of sound at throat	1116 m/s
Throat pressure	12.75 bar
Wall thickness	0.004 m
α-Aluminum / α-Stainless [6]	97.1e-6 / 13.4e-6 m^2/s
Diffusion time scale, Al	0.164 sec
Diffusion time scale, SS	1.19 sec

StarCCM+ Software Setup & Features

The actual part used in CFD simulation, shown below in Figure 2, was created in Solidworks using the geometry of the engine, however the leftmost portion containing the fuel injection manifold is removed to create a simpler surface to act as an inlet. The engine wall geometry is also modified by removing the structural honeycombing designed to support the bell. This change will affect the results by eliminating conduction through these fins, however it is expected that the engine will melt before fin cooling becomes important.

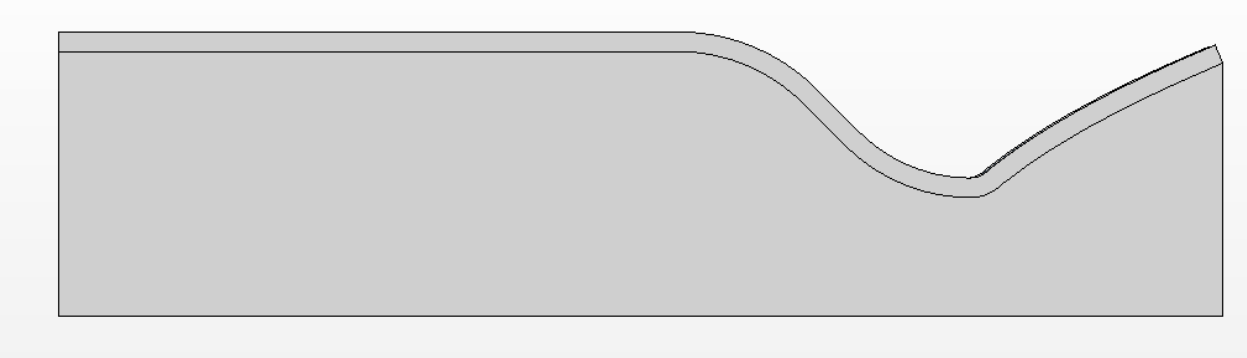

Figure 2: Part geometry used for StarCCM+ simulation. Dimension are identical to the model shown previously, with simplifications described in the text. The large, lower portion is the fluid region and the thin body on top is the solid region.

To simplify the model and reduce runtime, a 2D axisymmetric model is used to take advantage of the rotational symmetry of the part. With a flat model, the total number of cells is dramatically reduced compared to a 3D mesh with similar base size. This allows the model to run more quickly at a finer mesh size at the cost of less insight into three dimensional flow phenomena. Running on 4-cores in parallel, this simulation runs in approximately 10 minutes.

Model Selection

Because rocket mechanics require compressible flow, the fluid region is configured with ideal-gas-compressible and coupled flow models. Because of the Reynolds number, turbulence is expected, and so the K-ε turbulence model has also been selected. The Star help documentation suggests that K-ε turbulence model offers a good compromise between computation intensity and robustness including in scenarios which model heat transfer [7]. The wall of the engine is modeled with coupled solid energy and a constant density as only heat transfer is being considered at this time. Both regions use an implicit unsteady model with expert initialization turned on to simulate the transient heating of the engine wall.

Boundary Conditions

The two key boundary conditions in this simulation are the inlet and outlet conditions. The inlet of the engine, corresponding to the left surface in Figure 2, is modeled as a stagnation inlet with temperature and pressure from the engine parameters in Table 1. The outlet is configured as a pressure outlet with an ambient pressure of 1 bar. The interface between the two regions is set as a conjugate heat transfer boundary, and the initial wall temperature is set at 100K to reflect the system prechill with liquid Oxygen. All other conditions have been left at their default values.

CFD Mesh Setup

The mesh used for the fluid region is a 2D polyhedral mesh with a base size of 0.4mm and 5 prism layers. The surface growth rate for the fluid mesh is reduced to 1.1 to create a denser mesh in the throat and bell areas. The fluid region contains a total of 19,190 cells. The solid region is meshed with quadrilateral elements at a base size of 0.4mm, approximately 10% of the wall thickness, resulting in a mesh of 4,602 cells. Both meshes pass internal mesh diagnostic report with no invalid cells.

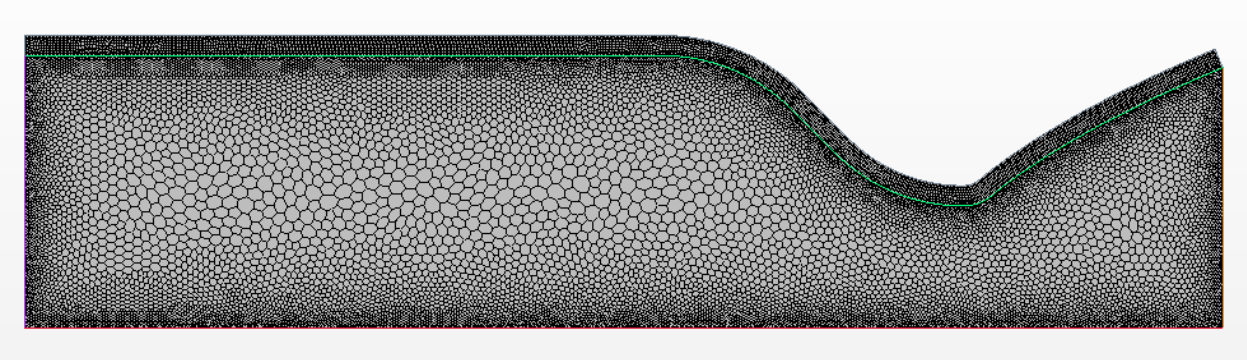

Figure 3: Final mesh of the fluid and solid regions. Both regions are meshed with a 0.4mm base size for a total of ~23,800 cells.

To better illustrate the sizes of the solid and fluid mesh, Figure 4 shows a zoomed-in view of the throat region of the engine. The green line is the contact boundary between the solid and fluid regions.

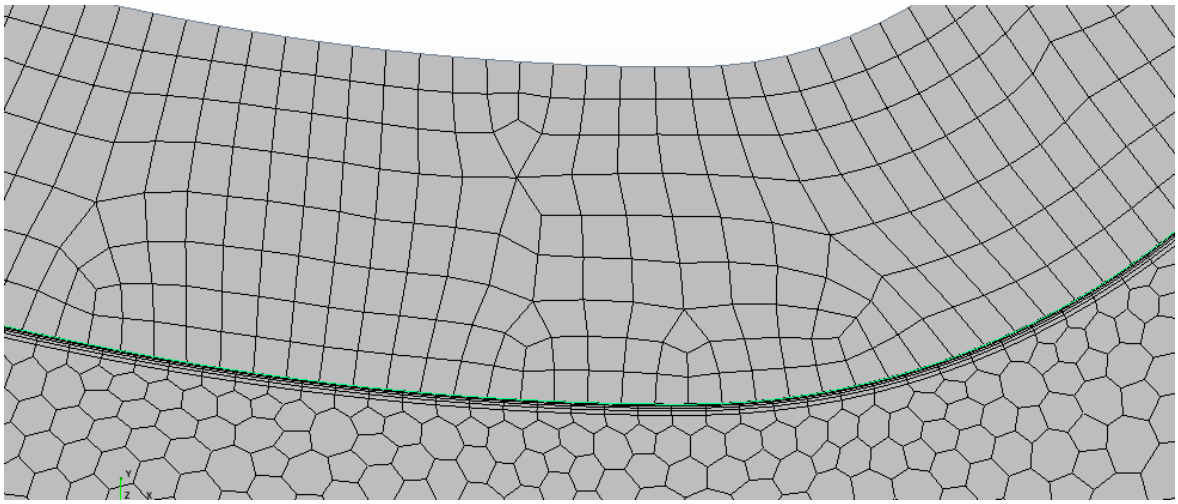

Figure 4: zoomed in mesh view of the throat region showing relative sizes of fluid and solid region meshes.

Results & Discussion

Model Validation

Before considering the temperature results, the model is first inspected to see how closely it matches the rocket design reference materials, basic compressible flow equations, and ensure that conjugate heat transfer is working. The first, and most basic, requirement of a rocket engine is that it should create choked flow at the throat and supersonic exhaust, shown below in Figure 5, which plots the Mach number and pressure values along the central axis of the engine.

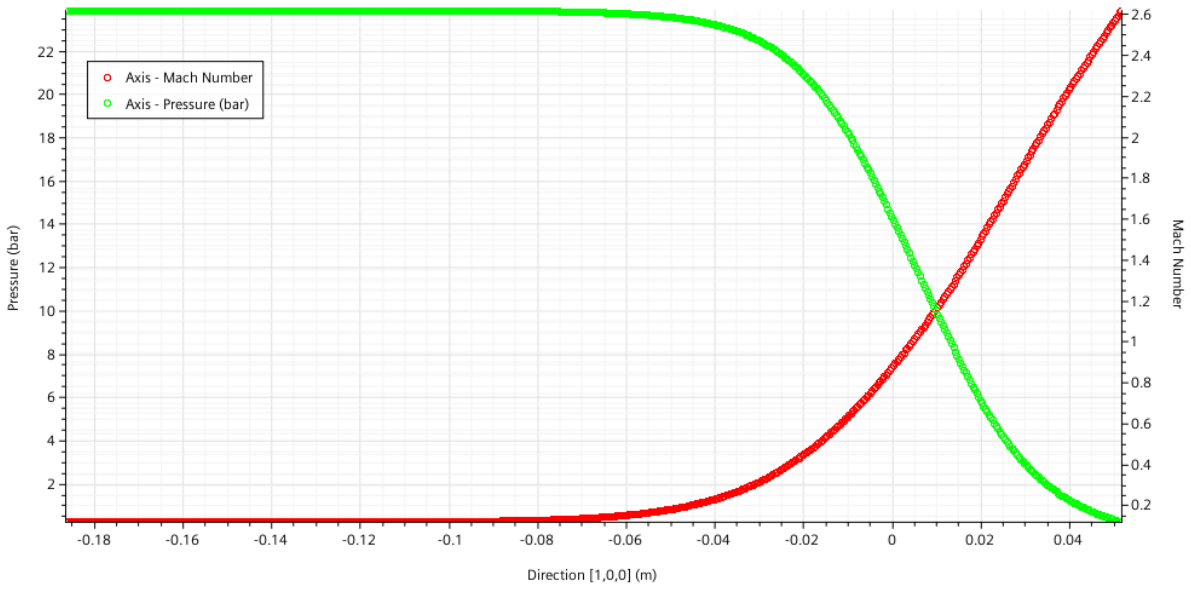

Figure 5: Mach number and pressure along the center axis. The zero-point is where the narrowest part of the engine occurs. The sonic transition at the axis is slightly downstream of the throat.

Seen in the plot above, when the red Mach number = 1, the green pressure line indicates a pressure of approximately 12.8 bar, which is close to the 12.75 bar calculated from the isentropic pressure ratio equation. Looking at the Mach number as a field in Figure 6 below, the actual shape of the sonic surface is that of a dome rather than flat as I originally anticipated. Upon further investigation, this shape

matches the Mach assumptions described in Huzel and shown in figure 4.13 (located in the Appendix). The nonuniform exhaust velocities are also similar to those described by Huzel in the same section.

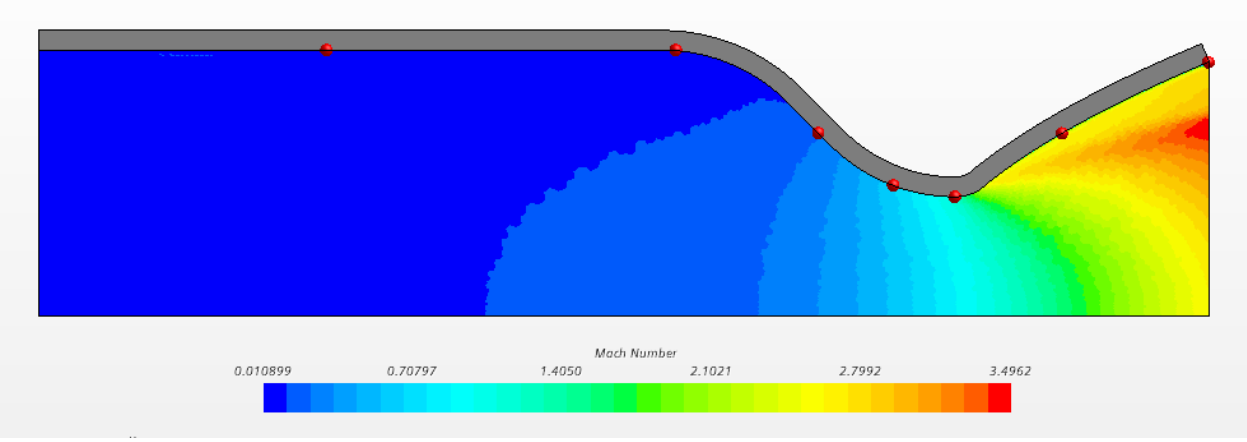

Figure 6: Mach number field through engine section. This field is from the Stainless Steel model run however the flow field is identical for both engine material types.

To confirm that conjugate heat transfer is working as expected, Figure 7 shows the temperature field through the fluid and solid regions of the stainless steel model. Huzel & Huang state in chapter 4 that the highest heat flux is experienced in the throat, and this behavior can be seen in the scalar scene below where the lightest wall colors occur just upstream of the throat. There is also a light spot at the very left edge of the wall, however this is likely an artifact of how the engine was truncated to simplify the inlet surface rather than a real phenomenon. In the real engine, the fuel injector will be located in the center of the engine, so the inlet hotspot seen below would not exist.

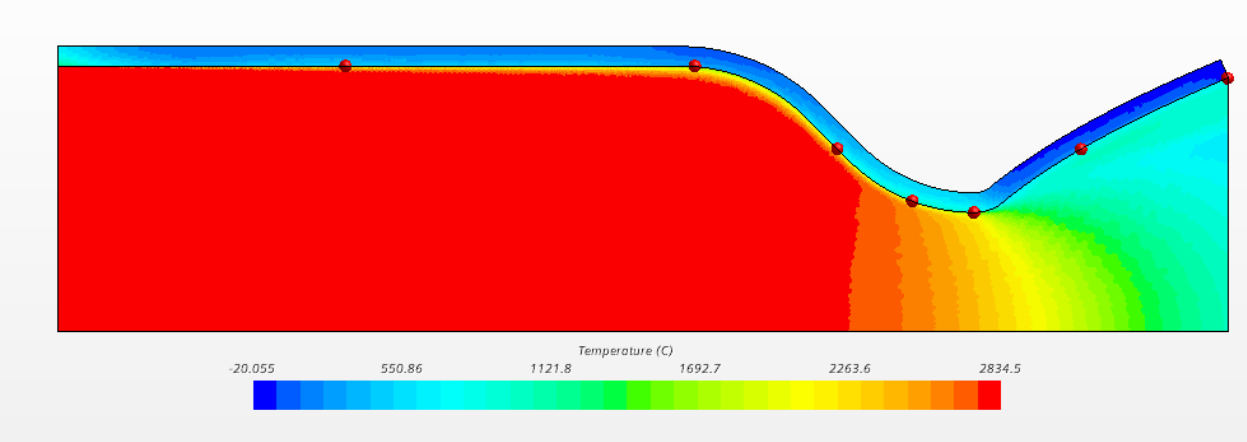

Figure 7: Temperature field of the 316SS model after 3.0s of elapsed time. The wall shows heating concentrated at the entrance and contraction region just upstream of the throat.

The temperature scene also shows the development of a boundary layer of cooler gas. The gas temperature is prescribed at the inlet on the left side, so the gas cools as it flows through the engine. This is expected, however it is also a potential source of model error. There will certainly be boundary layer formation in the actual engine, however with combustion occurring throughout the engine chamber, the boundary layer may differ from that formed in this model.

The final model validation test is a mass flow report. A good model will show only a small difference (ideally zero) between the mass flow in and out. As Figure 8 shows, the model has only a 2e-5 kg/s

difference between the amount of air flowing in and flowing out, or a model error of about 0.004% of the flow rate.

Mass Flow

Part	Value (kg/s)
fluid_region: Body2.inlet	-5.287026e-01
fluid_region: Body2.outlet	5.287263e-01
Total:	2.368974e-05

Figure 8: Mass flow report showing the error in the model's continuity equation.

Surface Temperature: Aluminum-walled Engine

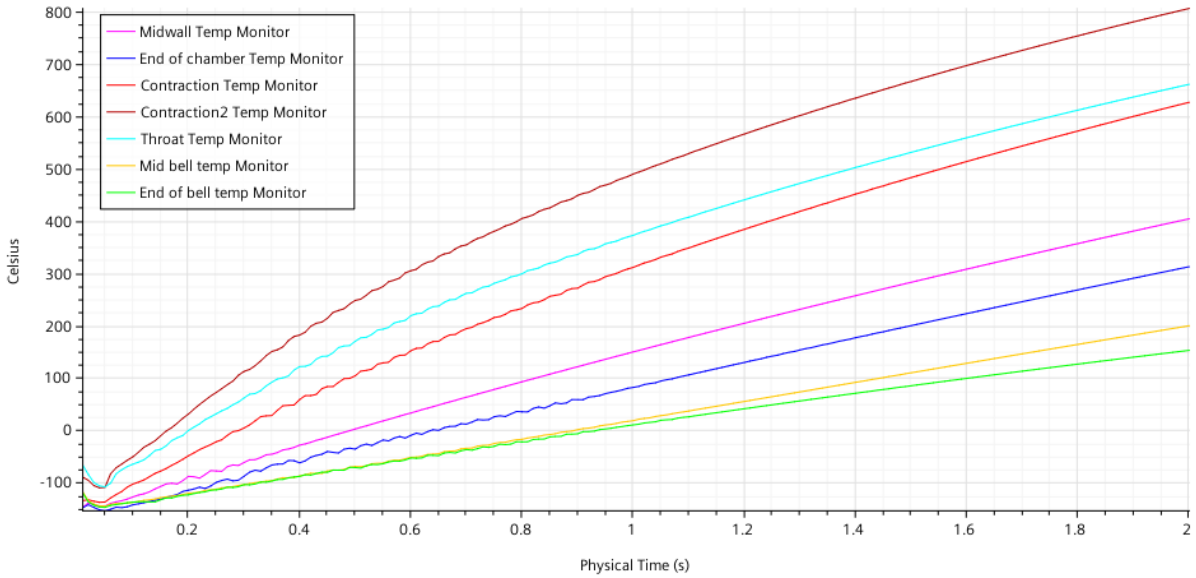

Figure 9: Metal surface temperature for the Aluminum engine wall. The temperature probe points plotted in this graph are the dots shown in Figure 5, ordered in the legend as they appear in Figure 5 from left to right.

For 6061 Aluminum alloy, its liquidus temperature is 580°C [8]. The Contraction2 probe in Figure 9 reaches this wall temperature after approximately 1.25 seconds of simulated engine firing. The engine wall is even being modeled with an initial temperature of 100K to account for the engine prechill with liquid Oxygen, however the difference between an ambient and a chilled temperature start is less than 0.1 seconds before the melting temperature is reached. One surprising result of this run is that the wall in the middle of the combustion chamber heats much slower than the contraction region, only reaching 400°C by the end of the 2 second model run. The large discrepancy between the hottest and coldest temperature probes suggest that an overall surface average of the wall heat transfer would produce inaccurate results, and instead the focus should be on the specific regions that experience the highest heat flux.

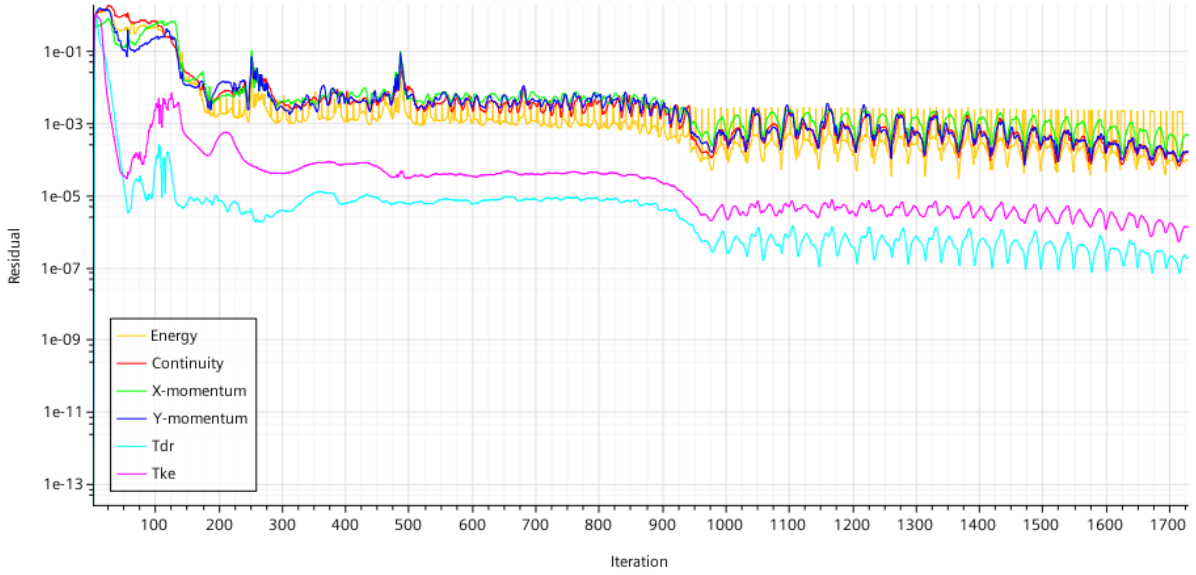

Figure 10: Residuals plot for the Aluminum engine run. The smallest periodic oscillations of the residuals indicate the next time step. The reason for the longer periodic oscillations is unknown.

Surface Temperature: Stainless Steel-walled Engine

Below in Figure 11 and Figure 12 are the model results for the stainless steel model run. The only differences between this model and the prior model run are the change of wall material and the extension of the physical time to 3.0s from 2.0s. Interestingly, the time to reach 500°C for the stainless steel engine is actually faster for the stainless steel model at 0.9s compared to the Aluminum's 1.0s. The primary difference between the two models is that the melting point of 316 Stainless Steel is approximately 1400°C, so there is significantly a greater buffer before the surface melts.

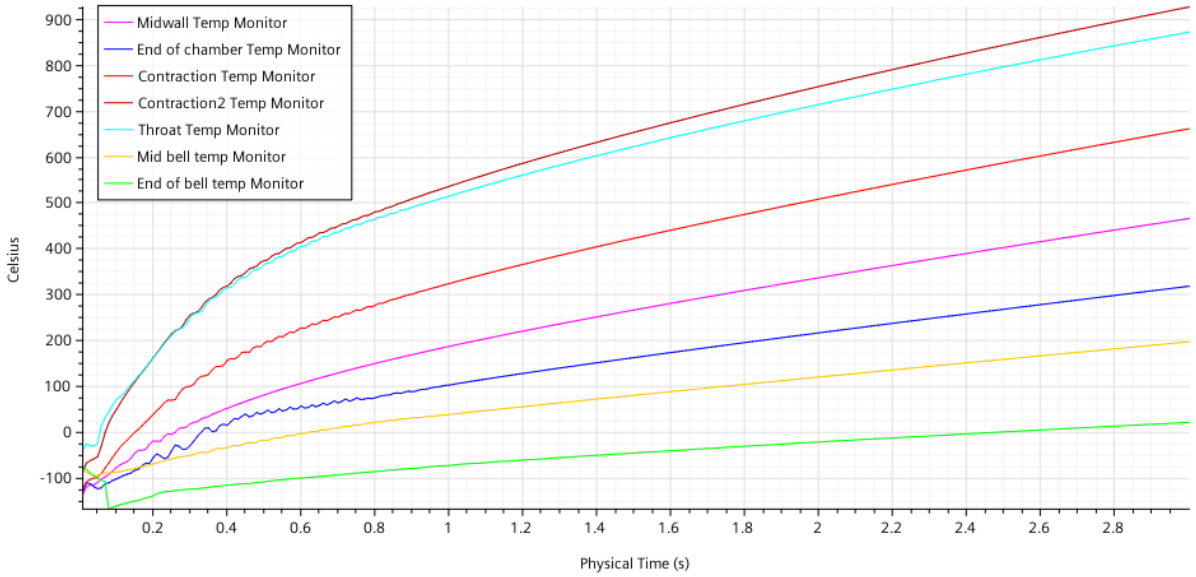

Figure 11: Surface temperature graph for the stainless steel rocket wall. Temperature probes are unchanged from those for the Aluminum walled rocket.

As can be seen, even with the run time extended to 3 seconds, the highest temperature experienced by the stainless steel wall at the Contraction2 probe is 900°C, which is still 500°C below the melting point of

the metal. This should allow enough buffer that the engine could be fired for several seconds without melting.

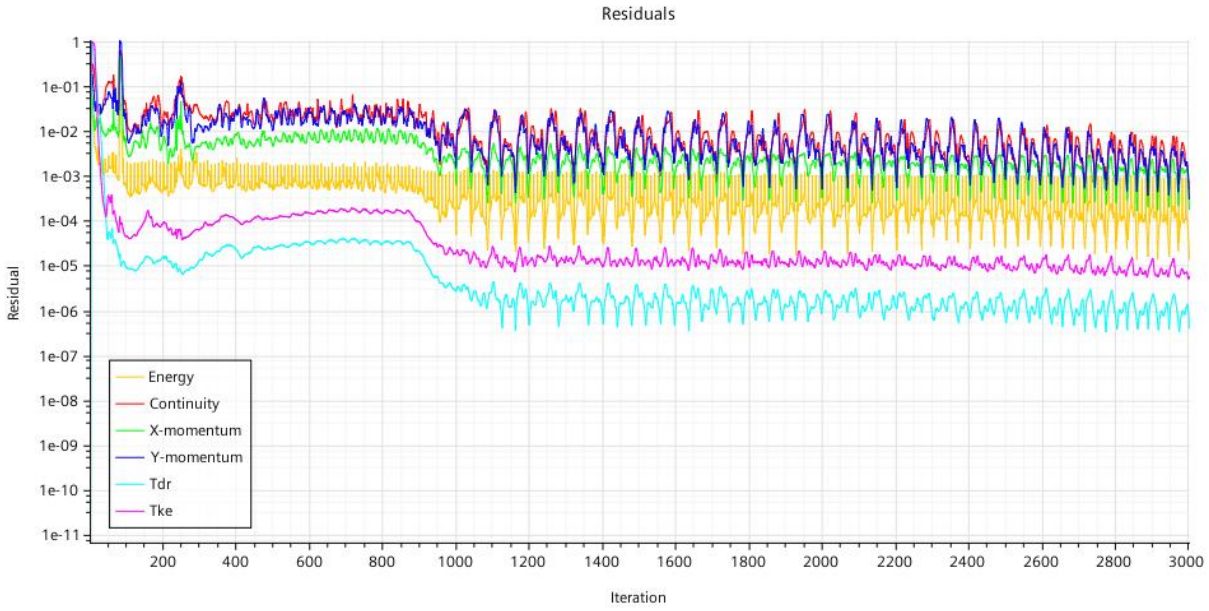

Figure 12: Residuals for the stainless steel rocket. The smallest scale oscillations are due to the inner iterations at each time step. The cause of the larger oscillations is unknown.

Conclusion

Based on the two model runs shown above, stainless steel is superior to Aluminum for a heat sink rocket engine. While Aluminum has a thermal conductivity 17 times higher than 316 stainless steel [6], this increased conductivity is clearly overwhelmed by the convective heat transfer from the gas to the wall, illustrated by both metals sharing a similar heating curve. The stainless steel actually initially heats slightly faster than the Aluminum, which may be due to the lower specific heat of steel compared with Aluminum. Regardless, the advantage of stainless steel, at least for a heat sink engine, is its melting point of 1400°C. This heat tolerance allows the temperature of the wall to rise much closer to the temperature of the gas boundary layer, reducing the ΔT between the wall and fluid and slowing heat transfer. PSAS would like to conduct a test fire of approximately 3 seconds, and based on the results of this study, only a stainless steel design can be expected to survive.

Given additional time and resources, three areas where I would look to improve the model are the inlet conditions, the wall boundary layers and active cooling. While the stagnation inlet condition with hot air does produce a sonic transition and supersonic exhaust flow, Figure 8 predicts a flow rate of 0.58 kg/s. In contrast, the rocket equations in Huzel and the PSAS optimization scripts predicts a combined fuel/oxidizer mass flowrate of 2.6 kg/s, over four times great. I did rerun the model once with a mass flowrate inlet condition at the PSAS prescribed value and this produced a chamber pressure of 120 bar, well above the engine design pressure. It's not clear why the CFD model predicts a mass flow rate so much lower than the theoretical rocket equations, however this discrepancy merits further investigation.

The second are I would improve with more time is the boundary layer behavior of the rocket. As mentioned earlier, the current model prescribes a temperature at the inlet, but then allows the temperature of the fluid to fall as it travels through the engine. This forms a cooler boundary layer as the gas progresses down the chamber wall. In a combustion process, the temperature of the inside of the engine chamber will be determined by the heat and mass balance of the system as it burns, so this may produce different boundary layer behavior than currently modeled. Additionally, the fuel injection system will be spraying liquid droplets into the engine, so in the fraction of a second before ignition, a fluid film would likely form on the inner surface of the engine which could act as an insulator as it boils off.

Finally, the design specification of LV-4 will require an engine burn time of approximately 30-45 seconds. Clearly neither an Aluminum nor stainless steel engine will survive a burn of that duration if it is uncooled. The addition of active cooling modeling would be a very useful extension of this simulation. This addition would likely require the conversion from axisymmetric to fully three-dimensional modeling to allow for investigation of different cooling channel geometries. If completed, however, a conjugate heat transfer model with active cooling would allow for virtual testing of engine designs before prototyping. Because PSAS is typically a budget-limited organization, an effective CFD model would have the potential to reduce cost and increase the potential for success by allowing for testing and design iteration before prototyping.

References

[1] D. Huzel and D. Huang, Modern Engineering for Design of Liquid-Propellant Rocket Engines, Washington: American Institute of Aeronautics and Astronautics, 1992.

[2] "Parametric LFE Generation and Analysis," 16 March 2020. [Online]. Available: https://github.com/psas/liquid-engine-analysis/tree/master/LFE%20Design.

[3] E. Rathakrishnan, Instrumentation, Measurements, and Experiments in Fluids, Boca Raton: CRC Press, 2007.

[4] B. Munson, T. Okiishi, W. Huebsch and A. Rothmayer, Fundamentals of Fluid Mechanics, 7th ed, Hoboken: John Wiley & Sons, 2013.

[5] "Universal and Individual Gas Constants," 2020. [Online]. Available: https://www.engineeringtoolbox.com/individual-universal-gas-constant-d_588.html.

[6] F. Incropera and D. Dewitt, Fundamentals of Heat and Mass Transfer, 7th ed, Hoboken: John Wiley & Sons, 2011.

[7] "Deciding on a RANS Turbulence Model," 16 March 2020. [Online].

[8] Aerospace Specification Metals, Inc., "6000 Series Aluminum Alloys," n.d.. [Online]. Available: http://asm.matweb.com/search/SpecificMaterial.asp?bassnum=MA6061T6.

Appendix

The figure below is from Huzel & Huang chapter 4 in discussing the behavior of rocket engine bells. The line T-O in the figure is described as the assumed Mach line through the engine bell. This bowed surface closely matches the simulation results found in Figure 6.

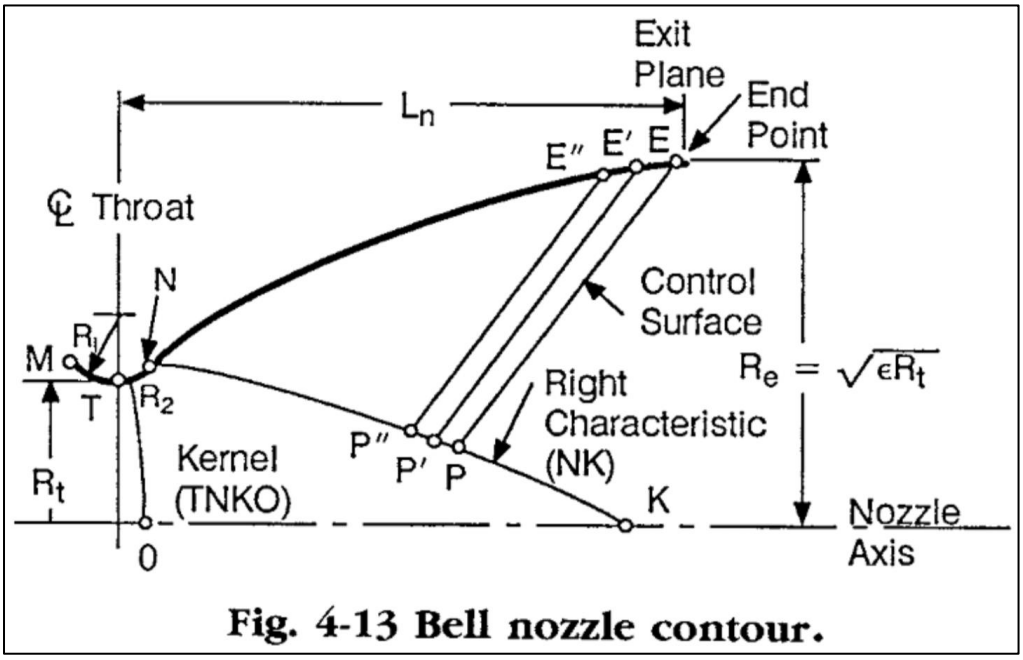

Figure 13: from Huzel & Huang chapter 4, illustrating the bell contours.

When the stainless steel model time is extended, the simulation predicts melting will occur after approximately seven seconds, nearly 6 seconds longer than predicted melting for the Aluminum engine.

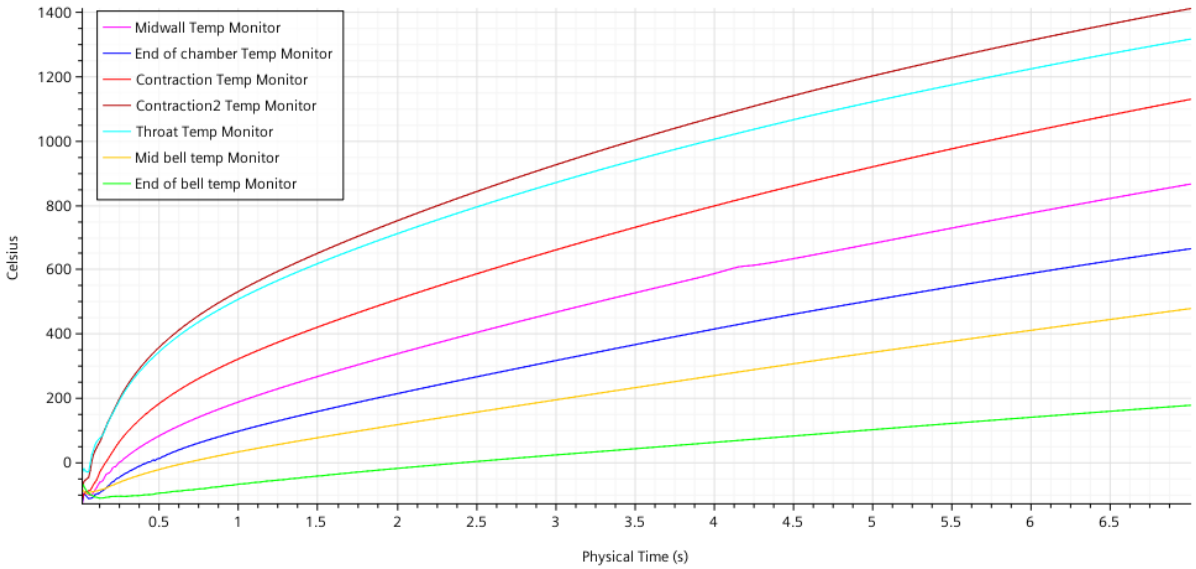

Figure 14: Stainless steel model with the stopping criterion extended to 7 seconds of physical time.

The following is an example of the outputs from CEARun, used in designing the prototype engine:

```
       NASA-GLENN CHEMICAL EQUILIBRIUM PROGRAM CEA2, FEBRUARY 5, 2004
                    BY  BONNIE MCBRIDE AND SANFORD GORDON
     REFS: NASA RP-1311, PART I, 1994 AND NASA RP-1311, PART II, 1996

*******************************************************************************


### CEA analysis performed on Wed 20-Nov-2019 17:33:36

# Problem Type: "Rocket" (Infinite Area Combustor)

prob case=l337___________3510 ro equilibrium

# Pressure (1 value):
p,psia= 350

# Oxidizer/Fuel Wt. ratio (1 value):
o/f= 1.3

# You selected the following fuels and oxidizers:
reac
fuel C3H8O,2propanol   wt%= 64.8000  t,k= 419.150
fuel H2O(L)            wt%= 35.2000  t,k= 419.150
oxid O2(L)             wt%=100.0000


### IMPORTANT:  The following line is the end of your CEA input file!
end

             THEORETICAL ROCKET PERFORMANCE ASSUMING EQUILIBRIUM

          COMPOSITION DURING EXPANSION FROM INFINITE AREA COMBUSTOR

Pin =   350.0 PSIA
CASE = l337___________

            REACTANT                    WT FRACTION      ENERGY      TEMP
                                         (SEE NOTE)     KJ/KG-MOL      K
FUEL        C3H8O,2propanol              0.6480000   -260183.607    419.150
FUEL        H2O(L)                       0.3520000   -276642.895    419.150
OXIDANT     O2(L)                        1.0000000    -12979.000     90.170

O/F=    1.30000  %FUEL= 43.478261  R,EQ.RATIO= 1.141548  PHI,EQ.RATIO= 1.194371

                CHAMBER   THROAT
Pinf/P            1.0000   1.7258
P, BAR            24.132   13.983
T, K             3097.82  2946.38
RHO, KG/CU M    2.1733 0 1.3380 0
H, KJ/KG        -3799.20 -4387.14
U, KJ/KG        -4909.58 -5432.21
G, KJ/KG        -40150.9 -38961.7
S, KJ/(KG)(K)    11.7346  11.7346

M, (1/n)          23.196   23.441
(dLV/dLP)t      -1.02241 -1.01779
(dLV/dLT)p        1.4656   1.3897
Cp, KJ/(KG)(K)    5.7638   5.3086
GAMMAs            1.1251   1.1252
SON VEL,M/SEC     1117.7   1084.4
MACH NUMBER        0.000    1.000
```

PERFORMANCE PARAMETERS

Ae/At	1.0000
CSTAR, M/SEC	1663.3
CF	0.6520
Ivac, M/SEC	2048.1
Isp, M/SEC	1084.4

MASS FRACTIONS

*CO	0.17619	0.16525
*CO2	0.34213	0.35933
COOH	0.00001	0.00000
*H	0.00045	0.00036
HO2	0.00005	0.00003
*H2	0.00509	0.00481
H2O	0.42670	0.43334
H2O2	0.00001	0.00000
*O	0.00259	0.00172
*OH	0.02769	0.02138
*O2	0.01909	0.01377

* THERMODYNAMIC PROPERTIES FITTED TO 20000.K

NOTE. WEIGHT FRACTION OF FUEL IN TOTAL FUELS AND OF OXIDANT IN TOTAL OXIDANTS